International Journal of Digital Information and Wireless Communications (IJDIWC) 4(2): 213-225
The Society of Digital Information and Wireless Communications, 2014 (ISSN: 2225-658X)

Robust Nonlinear Composite Adaptive Control of Quadrotor

Bara J. Emran[1] and Aydin Yesildirek[2]
[1]With the Mechatronics Graduate Program
[2]Associate Professor with the Department of Electrical Engineering
[1,2]American University of Sharjah, UAE
[1] Bara.Emran@yahoo.com, [2]Ayesildirek@aus.edu

ABSTRACT

A robust nonlinear composite adaptive control algorithm is done for a 6-DOF quadrotor system. The system is considered to suffer from the presence of parametric uncertainty and noise signal. The under-actuated system is split to two subsystems using dynamic inversion. A sliding mode control is controlling the internal dynamics while the adaptive control is controlling the fully actuated subsystem. All the plant parameters such as mass, system inertia, thrust and drag factors are considered as fully unknown and vary with time. The composite adaptive control is driven using the information from two errors; tracking error and prediction error. An enhancement on the adaptive control has been done using robust technique to reject the presence of the noise. The stability of the closed-loop system is driven in the flight region of interest. Also the performance of the designed controller is illustrated to follow a desired position, velocity, acceleration and the heading angle of quadrotor despite the fully unknown parameters and noise measurement.

KEYWORDS

Nonlinear Quadrotor Control, Under-Actuated system, Composite Adaptive Control, Unknown Parameters, Robust Control.

1 INTRODUCTION

A lot of interest in developing a control algorithm for quadrotor has been grown lately; this is because of its low cost, the high ability for maneuver and vertically teak off and landing which make it very popular as a research platform especially for indoor applications [1]-[5].

However, Quadrotors, like several different dynamic systems to be controlled, have unknown or slowly varying parameters. This problem could make such systems unstable and harder to be controlled. As an example, firefighting air craft suffer from considerable mass changes as they load or unload large quantities of water.

Adaptive control is an admirable candidate for this type of systems because of its capability of tracking a desired output signal with the presence of parametric uncertainties. As explanation, if the plant parameters are exactly known, the controller should make the plant output matching to that of the reference model. However, if they are not known, the adaptive law adjusts the controller parameters to achieve an acceptable convergence to desired output tracking. It is important to mention that, the convergence of the parameters to the exact value depends on the richness of the input signal. In this paper, a so called model reference adaptive control (MRAC) method is used.

Another main problem related to the parametric uncertainties is parameter drift. Parameter drift is mainly caused by the measurement noise. And since the Adaptive law uses the measured output signal as information to adjust the control parameter, the presence of the noise signal will affect the adaptation mechanism. Thus, an enhancement to adaptive control has been done to make it more robust against the presence of the noise signal.

There are different parameters can be estimated using adaptive control scheme. Several proposed methods estimated only mass while the other estimated mass and inertia matrix. Still, very few researches took other parameters into accounts. In mass estimating, a backstepping approach has been done in [6] while an enhancement using adaptive integral backstepping has been done in [7]. An adaptive robust control has been used in [8] and a model reference adaptive control is done in [8]. However for mass and inertia estimating, a comparison between model reference adaptive control and model identification adaptive control has presented in [10]. Moreover a Lyapunov-based robust adaptive control has been used in [11], [12] and [13]. And in [14], a composite adaptive controller has been shown. Furthermore, estimating extra parameters such as aerodynamic coefficients can be shown first in [15] using Lyapunov-based robust adaptive control also in [16] using adaptive sliding mode control and last in [17] using adaptive integral backstepping method.

Quadrotor is considered as under actuated subsystem; it has more degree of freedom than number of actuators. Thus, the introduced control method will divide the whole system to two sub systems. The first subsystem will control the internal dynamics using sliding mode control. However, the second subsystem, which is a full actuated system, will be controlled using a robust adaptive control; to remove the effects of the parameter uncertainty and reject the noise while tracking the desired output.

This research paper is organized as follows. In Section 2, the problem statement is defined. The dynamic equation of the quadrotor model and the reference frames are introduced in the next section3. The proposed adaptive control scheme is fully described in Section 4. Followed by The enhancement on the adaptive law using robust technique in Section 5. Finally, the validation of the proposed control is done using Simulation in last section.

2 PROBLEM DEFINITION

Quadrotor, like any other systems, suffers from parametric uncertainty; either totally unknown or vary with time. In addition, the presence of the measurement noise will add an extra difficulty to control the system. There are different ways to control such systems such as; robust controller and adaptive control. Robust control makes sure the closed loop control system remain stable in the presence of disturbance while adaptive control deals with parametric uncertainty without having any prior information about the parameter.

In this paper, a nonlinear control of a 6-DOF quadrotor to follow a desired position, velocity, acceleration and a heading angle despite the parameter uncertainty and measurement noise is aimed. The main plant parameters such as mass, system inertia, thrust and drag factors are considered as fully unknown and vary with time.

The quadrotor is considered as under-actuated system. Thus, to control it in 6DOF, a dynamic inversion technique to split the system into two sub systems is been done.

3 QUADROTOR MODEL

Quadrotor has 6DOF and four actuators placed in a cross configuration. Using a symmetrical design of the quadrotor allows for a centralization of the control systems and the payload. Each one of the four rotors is connected to a propeller and all the propellers' axes of rotation are parallel to each other. Also, all the propellers have fixed-pitch blades and their airflow downwards to get an upward lift. The left and the right propellers rotate clock wise, while the front and the rear one rotate counter-clockwise. Using an opposite pair's directions will balance the quadrotor and remove the need for a tail rotor. Consequently, the movements of the quadrotor are directly related to the propellers velocities.

3.1 Reference Frame:

Two main reference frames has been defined to state the motion of a 6 DOF rigid body. The frames are:

1) Earth inertial reference (E-frame)
2) Body-fixed reference (B-frame).

The earth-frame is defined as an inertial right-hand reference and denoted by (o_E, x_E, y_E, z_E). Using this frame, the linear position ($\boldsymbol{\Gamma^E}$ [m]) of the quadrotor and the Euler angles ($\boldsymbol{\Theta^E}$ [rad]) has been defined.

$$\boldsymbol{\Gamma}^{E} = \begin{bmatrix} x \\ y \\ z \end{bmatrix}, \qquad \boldsymbol{\Theta}^{E} = \begin{bmatrix} \phi \\ \theta \\ \psi \end{bmatrix} \tag{1}$$

where x, y and z represent the position of the center of the gravity of the quadrotor in E-frame. While ϕ, θ and ψ represent the Euler angles in E-frame denoted by roll, pitch and yaw respectively.

The body-frame is considered as a right-hand reference denoted by (o_B, x_B, y_B, z_B). And it is attached to the body of the quadrotor. The torques (τ^B [Nm]) and the forces (F^B [N]) has been defined using this frame. See Figure 1.

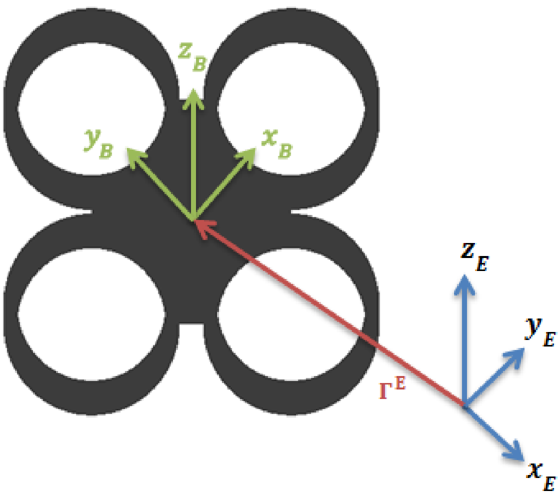

Figure 1: Quadrotor Reference Frames

To map the orientation of a vector from B-frame to E-frame and vice versa, a rotation matrix is needed and it is described as follows:

$$\boldsymbol{R_\Theta} = \begin{bmatrix} c_\psi c_\theta & s_\psi c_\theta & -s_\theta \\ -s_\psi c_\phi + c_\psi s_\theta s_\phi & c_\psi c_\phi + s_\psi s_\theta s_\phi & c_\theta s_\phi \\ s_\psi s_\phi + c_\psi s_\theta c_\phi & -c_\psi s_\phi + s_\psi s_\theta c_\phi & c_\theta c_\phi \end{bmatrix}$$

where c_x means $\cos(x)$ and s_x means $\sin(x)$.

3.2 Dynamic Equation:

Using the rotation matrix to map the forces and the torques from the body frame to the earth frame and by using Euler-Lagrange approach, the dynamic equation of the quadrotor is driven and described as following:

$$\begin{bmatrix} \ddot{x} \\ \ddot{y} \\ \ddot{z} \end{bmatrix} = \frac{k}{m} \begin{bmatrix} s_\psi s_\phi + c_\psi s_\theta c_\phi \\ -c_\psi s_\phi + s_\psi s_\theta c_\phi \\ c_\theta c_\phi \end{bmatrix} u - \begin{bmatrix} 0 \\ 0 \\ g \end{bmatrix} \tag{2}$$

$$\begin{bmatrix} \ddot{\phi} \\ \ddot{\theta} \\ \ddot{\psi} \end{bmatrix} = \begin{bmatrix} \left(\frac{I_y - I_z}{I_x}\right)\dot{\theta}\dot{\psi} \\ \left(\frac{I_z - I_y}{I_y}\right)\dot{\phi}\dot{\psi} \\ \left(\frac{I_x - I_y}{I_z}\right)\dot{\phi}\dot{\theta} \end{bmatrix} + \begin{bmatrix} \frac{J_p}{I_x}\dot{\theta} \\ \frac{J_p}{I_x}\dot{\phi} \\ 0 \end{bmatrix} \Omega + \begin{bmatrix} \frac{k}{I_x} & 0 & 0 \\ 0 & \frac{k}{I_y} & 0 \\ 0 & 0 & \frac{d}{I_z} \end{bmatrix} \begin{bmatrix} \tau_\phi \\ \tau_\theta \\ \tau_\psi \end{bmatrix} \tag{3}$$

where the inputs are defined as:

$$\begin{bmatrix} u \\ \tau_\phi \\ \tau_\theta \\ \tau_\psi \end{bmatrix} = \begin{bmatrix} 1 & 1 & 1 & 1 \\ -l & 0 & l & 0 \\ 0 & l & 0 & -l \\ 1 & -1 & 1 & -1 \end{bmatrix} \begin{bmatrix} f_1 \\ f_2 \\ f_3 \\ f_4 \end{bmatrix} \tag{4}$$

$$f_i = w_i^2$$

$$\Omega = w_1 - w_2 + w_3 - w_4$$

where I_x, I_y and I_z are the quadrotor inertia matrix around x, y and z axis respectively in [N·m·s^2], m is the quadrotor mass in [kg], Ω is the overall propellers' speed in [rad·s^{-1}], J_p is the total rotational moment of inertia around the propeller axis in [N·m·s2], k is the thrust factor in [N·s^2], d is the drag factor in [N·m·s^2], l is the distance between the center of the quadrotor and the center of a propeller in [m], $[u, \tau_\phi, \tau_\theta, \tau_\psi]^T$ are the inputs of the quadrotor representing the collective force, roll torque, pitch torque, yaw torque respectively and w_i is the speed of the ith motor in [rad·s^{-1}].

4 CONTROL SCHEME

Because of presence of the under-actuated problem, reaching any desired set-point in space is not possible for quadrotor. Thus to achieve tracking control for the desired command $[x_c, y_c, z_c, \psi_c]$, a dynamic inversion method is been used to divide the system into two subsystems [18].

The internal dynamics that yield from using the feedback linearization are considered in the first subsystem and it is given by:

$$\begin{bmatrix} \ddot{x} \\ \ddot{y} \end{bmatrix} = \frac{k}{m} \begin{bmatrix} s_\psi s_\phi + c_\psi s_\theta c_\phi \\ -c_\psi s_\phi + s_\psi s_\theta c_\phi \end{bmatrix} u \qquad (5)$$

A sliding mode control has been used to control the first subsystems and to generate the command signal $[\phi_c , \theta_c]$.

However, the second subsystem is considered as a full actuated system and it is defined as:

$$\begin{bmatrix} \ddot{z} \\ \ddot{\phi} \\ \ddot{\theta} \\ \ddot{\psi} \end{bmatrix} = \begin{bmatrix} -g \\ \left(\frac{I_y - I_z}{I_x}\right)\dot{\theta}\dot{\psi} \\ \left(\frac{I_z - I_x}{I_y}\right)\dot{\phi}\dot{\psi} \\ \left(\frac{I_x - I_y}{I_z}\right)\dot{\phi}\dot{\theta} \end{bmatrix} + \begin{bmatrix} \frac{k}{m} & 0 & 0 & 0 \\ 0 & \frac{k}{I_x} & 0 & 0 \\ 0 & 0 & \frac{k}{I_y} & 0 \\ 0 & 0 & 0 & \frac{d}{I_z} \end{bmatrix} \begin{bmatrix} u_z \\ \tau_\phi \\ \tau_\theta \\ \tau_\psi \end{bmatrix} \qquad (6)$$

An adaptive control is been developed to control the second subsystem and to overcome the unknown parameters. In addition, the adaptive control is designed to achieve attitude and the altitude control of the quadrotor $[z, \phi , \theta , \psi]$. Furthermore, the adaptive control has been improved by using a robust techniques. Those Improvements have been introduced to improve the parameters estimation and noise rejection. The below block diagram in Figure 2 shows the overall control scheme.

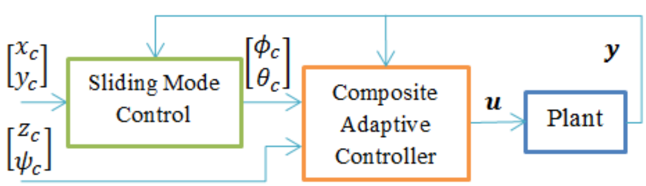

Figure 2: Control Scheme Block Diagram

4.1 Sliding Mode Control for Internal Dynamics:

To guarantee the stability of dynamic inversion technique, it is essential to stabilizing the internal dynamics of the system. As a result, a proper command ϕ_c and θ_c for the roll and pitch signals respectively are been selected such that the tracking control for x_c and y_c are been achieved. Thus, the internal dynamics will be grantee to be stable. The block diagram of the sliding control is shown in Figure 3.

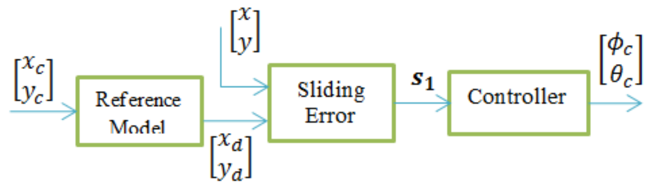

Figure 3: Sliding Control Block Diagram for the Internal Dynamics

The states of the first subsystem are defined as follow

$$\boldsymbol{q_1} = [x \quad y]^{\boldsymbol{T}} \qquad (7)$$

Let us rewrite internal dynamics equation in (5) as:

$$\ddot{\boldsymbol{q}}_1 = \frac{\bar{k}}{m} u \, \boldsymbol{\Psi} \begin{bmatrix} s_\phi \\ s_\theta \end{bmatrix}$$

$$\boldsymbol{\Psi} = \begin{bmatrix} s_\psi & c_\psi c_\phi \\ -c_\psi & s_\psi c_\phi \end{bmatrix} \qquad (8)$$

where the yaw angle (ψ) and the roll angle (ϕ) in the matrix $\boldsymbol{\Psi}$ are the current angles of the system. It is important to note that the matrix $\boldsymbol{\Psi}$ is invertible in the region of interest

$$\Delta_{\boldsymbol{\Psi}} = (s_\psi s_\psi c_\phi) - (-c_\psi c_\psi c_\phi)$$

$$\Delta_{\boldsymbol{\Psi}} = c_\phi \neq 0, \qquad -\frac{\pi}{2} < \phi < \frac{\pi}{2} \qquad (9)$$

4.1.1 Reference Model:

The desired trajectory for the first subsystem is been defined using the following reference model in state space form:

$$\frac{d}{dt}\begin{bmatrix}\boldsymbol{q}_{1_d}\\ \dot{\boldsymbol{q}}_{1_d}\end{bmatrix} = \boldsymbol{A}_{m1}\begin{bmatrix}\boldsymbol{q}_{1_d}\\ \dot{\boldsymbol{q}}_{1_d}\end{bmatrix} + \boldsymbol{B}_{m1}\,\boldsymbol{q}_{1_c} \tag{10}$$

$$\boldsymbol{q}_{1_c} = [x_c, y_c]^T$$

Where x_c and y_c represent the command inputs of the first subsystem and $\mathbf{A}_{m1}$ and $\boldsymbol{B}_{m1}$ represent the desired system performance.

4.1.2 Tracking and Sliding Mode Error:

Let the definition of the tracking error on XY-plane is calculated as:

$$\boldsymbol{e}_1 = \boldsymbol{q}_1 - \boldsymbol{q}_{1_d} = \begin{bmatrix}e_x\\ e_y\end{bmatrix} = \begin{bmatrix}x - x_d\\ y - y_d\end{bmatrix} \tag{11}$$

And the associated sliding mode error is defined as:

$$\boldsymbol{s_1} = \dot{\boldsymbol{e}}_\mathbf{1} + \boldsymbol{\Lambda}_\mathbf{1}\boldsymbol{e}_\mathbf{1}$$

$$\boldsymbol{s_1} = \begin{bmatrix}s_x\\ s_y\end{bmatrix} = \begin{bmatrix}\dot{e}_x\\ \dot{e}_y\end{bmatrix} + \begin{bmatrix}\lambda_x\, e_x\\ \lambda_y\, e_y\end{bmatrix} \tag{12}$$

$$\boldsymbol{\Lambda}_\mathbf{1} = diag([\lambda_x \quad \lambda_y]) > 0$$

where λ_x and λ_y are design positive constants and represent a stable Hurwitz polynomial.

4.1.3 Control Law:

A relation between the input force (u) and the gravitational acceleration (g) could be made by using the dynamic equation (1) to simplify the control law. From the dynamic equation of the z-axis:

$$\ddot{z} = \frac{k}{m}\, u\; cos(\phi)\, cos(\theta)\; - \; g \tag{13}$$

When the system moves in XY-plane, the acceleration in z-axis will equal to zero:

$$\ddot{z} = 0 \;\; \rightarrow \;\; \frac{k}{m}\, u\; cos(\phi)\, cos(\theta) \; = \; g \tag{14}$$

$$\frac{k}{m}\, u = \frac{g}{cos(\phi)\, cos(\theta)} = G \tag{15}$$

Thus the control law is defined in the form of:

$$\begin{bmatrix}\phi_c\\ \theta_c\end{bmatrix} = sin^{-1}(\boldsymbol{\Psi}^{-1}.\,[\ddot{\boldsymbol{q}}_{\boldsymbol{1_d}} - \boldsymbol{\Lambda}_1\dot{\boldsymbol{e}}_1 - \boldsymbol{K}_1\boldsymbol{s}_1]/G\,) \tag{16}$$

$$\boldsymbol{K}_1 = diag(k_x, k_y) > 0$$

where the constant k_x and k_y are design positive value and represent a stable Hurwitz polynomial. Substitute the control law in (5) yields:

$$\ddot{\boldsymbol{q}}_1 = \; \ddot{\boldsymbol{q}}_{1_d} - \boldsymbol{\Lambda}_1\dot{\boldsymbol{e}}_1 - \boldsymbol{K}_1\boldsymbol{s}_1$$

$$\dot{\boldsymbol{s}}_1 + \boldsymbol{K}_1\, \boldsymbol{s}_1 = \boldsymbol{0} \tag{17}$$

Therefore, this gives exponential convergence for $\boldsymbol{s}_1$ which guarantees the convergence of XY-plane tracking error ($\boldsymbol{e}_1$).

4.2 Composite Adaptive Controller

The Adaptive control of nonlinear systems has been well studied in [19]-13[21]. The adaptive control is been applied for the second subsystem to guarantee the convergence of the attitude and altitude tracking $[\,z, \phi\,, \theta\,, \psi]$. In other words, the objective of using the adaptive control is to make the output asymptotically tracks the desired output $\boldsymbol{q}_{2_d}(t)$ despite the presence of parametric uncertainty.

The composite adaptive law uses both information from the tracking error and the prediction error to extract and estimate the parameters [22]. The block diagram of the composite adaptive control is shown in Figure 4.

4.3 Parameterization:

Let us define the states for the second subsystem as:

$$\boldsymbol{q_2} = \; [z \quad \phi \quad \theta \quad \psi]^{\boldsymbol{T}} \tag{18}$$

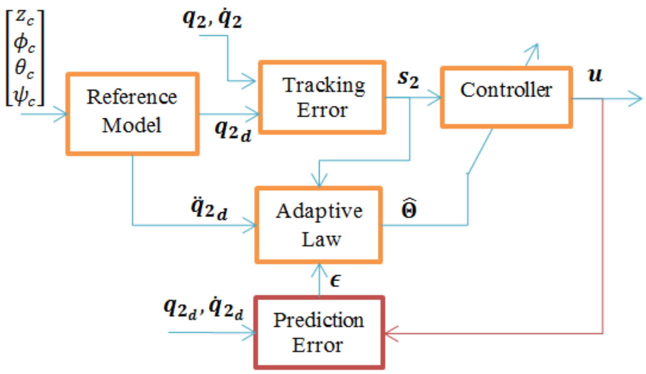

Figure 4: Composite Adaptive Control Block Diagram

By rewriting (6) in linear-in-parameter form yields:

$$\boldsymbol{\Phi\Theta} = \boldsymbol{u} \qquad (19)$$

$$\boldsymbol{\Theta} = \begin{bmatrix} \boldsymbol{\Theta_1} \\ \boldsymbol{\Theta_2} \end{bmatrix}, \qquad \boldsymbol{\Theta_1} = \begin{bmatrix} m/k \\ I_x/k \\ I_y/k \\ I_z/d \end{bmatrix}$$

$$\boldsymbol{\Theta_2} = \begin{bmatrix} I_z/k \\ (I_x - I_y)/d \end{bmatrix}$$

$$\boldsymbol{u} = [u \quad \tau_\phi \quad \tau_\theta \quad \tau_\psi]^{\boldsymbol{T}}$$

$$\boldsymbol{\Phi} = \boldsymbol{Q}(\ddot{q}_2) + \boldsymbol{F}(f_\phi, f_\theta, f_\psi, g)$$

$$\boldsymbol{Q} = \begin{bmatrix} \ddot{z} & 0 & 0 & 0 & 0 & 0 \\ 0 & \ddot{\phi} & 0 & 0 & 0 & 0 \\ 0 & 0 & \ddot{\theta} & 0 & 0 & 0 \\ 0 & 0 & 0 & \ddot{\psi} & 0 & 0 \end{bmatrix}$$

$$\boldsymbol{F}(f_\phi, f_\theta, f_\psi, g) = \begin{bmatrix} g & 0 & 0 & 0 & 0 & 0 \\ 0 & 0 & -f_\phi & 0 & f_\phi & 0 \\ 0 & f_\theta & 0 & 0 & -f_\theta & 0 \\ 0 & 0 & 0 & 0 & 0 & -f_\psi \end{bmatrix}$$

$$f_\phi = \dot{\theta}\dot{\psi}, \qquad f_\theta = \dot{\phi}\dot{\psi}, \qquad f_\psi = \dot{\phi}\dot{\theta}$$

4.3.1 Reference model

Similar to the previous subsystem, let the desired trajectory for the second subsystem been defined using the following reference model in state space form:

$$\frac{d}{dt}\begin{bmatrix} \boldsymbol{q}_{2_d} \\ \dot{\boldsymbol{q}}_{2_d} \end{bmatrix} = \boldsymbol{A}_{m2}\begin{bmatrix} \boldsymbol{q}_{2_d} \\ \dot{\boldsymbol{q}}_{2_d} \end{bmatrix} + \boldsymbol{B}_{m2}\,\boldsymbol{q}_{2_c} \qquad (20)$$

$$\boldsymbol{q}_{2_c} = [z_c, \phi_c, \theta_c, \psi_c]^{\boldsymbol{T}}$$

where $[z_c, \phi_c, \theta_c, \psi_c]$ represent the command inputs of the second subsystem and $\mathbf{A}_{m2}$ and $\boldsymbol{B}_{m2}$ represent the desired system performance Also.

4.3.2 Tracking and Sliding Mode Error:

Let the tracking error for second subsystem be calculated as:

$$\boldsymbol{e_2} = \boldsymbol{q_2} - \boldsymbol{q_{2_d}} = \begin{bmatrix} e_z \\ e_\phi \\ e_\theta \\ e_\psi \end{bmatrix} = \begin{bmatrix} z \\ \phi \\ \theta \\ \psi \end{bmatrix} - \begin{bmatrix} z_d \\ \phi_d \\ \theta_d \\ \psi_d \end{bmatrix} \qquad (21)$$

The associated sliding error is defined as :

$$\boldsymbol{s_2} = \begin{bmatrix} s_z \\ s_\phi \\ s_\theta \\ s_\psi \end{bmatrix} = \begin{bmatrix} \dot{e}_z \\ \dot{e}_\phi \\ \dot{e}_\theta \\ \dot{e}_\psi \end{bmatrix} + \begin{bmatrix} \lambda_z e_z \\ \lambda_\phi e_\phi \\ \lambda_\theta e_\theta \\ \lambda_\psi e_\psi \end{bmatrix} \qquad (22)$$

$$\boldsymbol{s_2} = \dot{\boldsymbol{e}}_2 + \boldsymbol{\Lambda_2 e_2}$$

$$\dot{\boldsymbol{s}}_2 = \ddot{\boldsymbol{e}}_2 + \boldsymbol{\Lambda_2}\dot{\boldsymbol{e}}_2 = \ddot{\boldsymbol{q}}_2 - \boldsymbol{q_r}$$

$$\boldsymbol{q_r} = \ddot{\boldsymbol{q}}_{2_d} - \boldsymbol{\Lambda_2}\,\dot{\boldsymbol{e}}_2$$

where $\boldsymbol{\Lambda_2}$ is a positive definite diagonal matrix defined as:

$$\boldsymbol{\Lambda_2} = diag([\lambda_z \quad \lambda_\phi \quad \lambda_\theta \quad \lambda_\psi]) \qquad (23)$$

And $[\lambda_z \quad \lambda_\phi \quad \lambda_\theta \quad \lambda_\psi]$ are design positive constant, which represent a stable Hurwitz polynomial.

4.3.3 Prediction Error:

The prediction error is assign as the difference between the actual input and the estimated control

$$\boldsymbol{\varepsilon} = \hat{\boldsymbol{u}} - \boldsymbol{u} = \boldsymbol{\Phi}\hat{\boldsymbol{\Theta}} - \boldsymbol{\Phi}\boldsymbol{\Theta} \tag{24}$$

Still, the presence of immeasurable acceleration in $\boldsymbol{\Phi}$ will prevent us from using this definition for the prediction error ($\boldsymbol{\varepsilon}$) directly for the parameter estimation. Thus, to avoid the appearance of the acceleration, a first order filter is used as follows:

$$\left[\frac{\lambda_f}{s+\lambda_f}\right] \boldsymbol{\Phi}(\ddot{\boldsymbol{q}}, f_\phi, f_\theta, f_\psi, g) = \boldsymbol{W}(\dot{\boldsymbol{q}}, f_\phi, f_\theta, f_\psi, g)$$
$$\lambda_f \left[\boldsymbol{Q}(\dot{\boldsymbol{q}}) - \frac{\lambda_f}{s+\lambda_f}\boldsymbol{Q}(\dot{\boldsymbol{q}}) + \frac{1}{s+\lambda_f}\boldsymbol{F}\right] = \boldsymbol{W} \tag{25}$$

where $\frac{\lambda_f}{s+\lambda_f}$ is stable filter with $\lambda_f > 0$.
Now, let us define a filtered prediction error ($\boldsymbol{\epsilon}$) as:

$$\boldsymbol{\epsilon} = \boldsymbol{W}\widetilde{\boldsymbol{\Theta}} = \boldsymbol{W}\widehat{\boldsymbol{\Theta}} - \boldsymbol{u}_1 \tag{26}$$

where $\mathbf{u_1}$ is the filtered version of the actual input, defined as:

$$\boldsymbol{u_1} = \left[\frac{\lambda_f}{s+\lambda_f}\right]\boldsymbol{u} \tag{27}$$

4.3.4 Control Law:

Let us define the control law as:

$$\boldsymbol{u} = \bar{\boldsymbol{\Phi}}\widehat{\boldsymbol{\Theta}} - \boldsymbol{K_2 s_2} \tag{28}$$

where:

$$\bar{\boldsymbol{\Phi}} = \boldsymbol{Q}(\boldsymbol{q_r}) + \boldsymbol{F}(f_\phi, f_\theta, f_\psi, g)$$
$$\boldsymbol{K_2} = diag(k_z, k_\phi, k_\theta, k_\psi) \tag{29}$$

where k_z, k_ϕ, k_θ and k_ψ are defined as design positive control gains. By substituting the control law in (6) yields:

$$\boldsymbol{\Phi\Theta} = \bar{\boldsymbol{\Phi}}\widehat{\boldsymbol{\Theta}} - \boldsymbol{K_2 s_2}$$
$$\boldsymbol{\Phi\Theta} = \bar{\boldsymbol{\Phi}}\widehat{\boldsymbol{\Theta}} - \boldsymbol{K_2 s_2} \pm \bar{\boldsymbol{\Phi}}\boldsymbol{\Theta} \tag{30}$$
$$(\boldsymbol{\Phi} - \bar{\boldsymbol{\Phi}})\boldsymbol{\Theta} + \boldsymbol{K_2 s_2} = \bar{\boldsymbol{\Phi}}(\widehat{\boldsymbol{\Theta}} - \boldsymbol{\Theta})$$

where $\widetilde{\Theta}$ is the parameter error defined by:

$$\tilde{\Theta} = \hat{\Theta} - \Theta \tag{31}$$

And by using the following simplification:

$$\Phi - \bar{\Phi} = Q(\ddot{q}) - Q(q_r) = Q(\dot{s_2})$$
$$\boldsymbol{Q}(\dot{\boldsymbol{s_2}})\boldsymbol{\Theta} = diag(\boldsymbol{\Theta_1})\dot{\boldsymbol{s}}_2 \tag{32}$$

The substitution of the control law in (6) become:

$$diag(\Theta_1)\,\dot{s_2} + K_2\, s_2 = \bar{\Phi}\tilde{\Theta} \tag{33}$$

Therefore, $\boldsymbol{s_2}$ converge exponentially to the region defined by ($\bar{\boldsymbol{\Phi}}\widetilde{\boldsymbol{\Theta}}$).

4.3.5 Adaptation Law:

To design a suitable adaptation law, let us define the Lyapunov function as:

$$V\left(s_1, s_2, \tilde{\theta}\right) = \frac{1}{2}\left[s_1^T H s_1 + s_2^T diag(\theta_1) s_2 + \tilde{\theta}^T P^{-1}\tilde{\theta}\right] \tag{34}$$

where the matrix $\mathbf{H}$, diag($\boldsymbol{\Theta_1}$) and $\mathbf{P}$ are symmetric positive definite. The derivative of the Lyapunov function can be calculated as:

$$\dot{V} = \boldsymbol{s_1}^{\boldsymbol{T}}\boldsymbol{H}\dot{\boldsymbol{s_1}} + \boldsymbol{s_2}^{\boldsymbol{T}} diag(\boldsymbol{\Theta_1})\,\dot{\boldsymbol{s_2}} + \dot{\tilde{\boldsymbol{\Theta}}}^T \boldsymbol{P}^{-1}\,\tilde{\boldsymbol{\Theta}} \tag{35}$$

Using the equation (17) and (33) yields:

$$\dot{V} = -\boldsymbol{s_1}^T\boldsymbol{K_1 s_1} - \boldsymbol{s_2}^T\boldsymbol{K_2 s_2} + \boldsymbol{s_2}^T\bar{\boldsymbol{\Phi}}\tilde{\boldsymbol{\Theta}} + \dot{\tilde{\boldsymbol{\Theta}}}^T\boldsymbol{P}^{-1}\widetilde{\boldsymbol{\Theta}} \tag{36}$$

By assuming constants or small time varying parameters ($\boldsymbol{\Theta}$):

$$\dot{\tilde{\boldsymbol{\Theta}}} = \dot{\hat{\boldsymbol{\Theta}}} - \dot{\boldsymbol{\Theta}} = \dot{\hat{\boldsymbol{\Theta}}} \tag{37}$$

Let us choose the composite adaptation law as:

$$\left(\boldsymbol{s_2}^T \bar{\boldsymbol{\Phi}} + \dot{\tilde{\boldsymbol{\Theta}}}^T \boldsymbol{P}^{-1} \right) \tilde{\boldsymbol{\Theta}} = 0$$
$$\dot{\tilde{\boldsymbol{\Theta}}} = -\boldsymbol{P}[\bar{\boldsymbol{\Phi}}^T \boldsymbol{s_2} + \boldsymbol{W^T R}(\boldsymbol{t})\boldsymbol{\epsilon}] \quad (38)$$

Thus, the derivative of the Lyapunov function (36) becomes:

$$\dot{V} = -\boldsymbol{s_1}^T \boldsymbol{K_1 s_1} - \boldsymbol{s_2}^T \boldsymbol{K_2 s_2} - \boldsymbol{\epsilon^T R}(\boldsymbol{t})\boldsymbol{\epsilon} \quad (39)$$

$$\dot{V} < 0$$

$$\boldsymbol{s_1}, \boldsymbol{s_2}, \boldsymbol{\epsilon} \to 0 \Rightarrow e_1, e_2 \to 0 \; as \; t \to \infty$$

By ysing Barbalat's lemma

$$\dot{e}_1, \dot{e}_2 \to 0$$

$$\tilde{\Theta} \; is \; bounded$$

And since $\boldsymbol{K_1}$ and $\boldsymbol{K_2}$ are positive definite diagonal matrices, the above expression guaranteed global stability and global tracking convergence of both the sliding control and adaptive control systems.

5 PARAMETER DRIFT

One of the major problems associated with parametric uncertainties is parameter drift. Parameter drift is mainly caused by measurement noise. To explain the parameter drift problem, let us consider a constant reference input. There is insufficient parameter information contained by constant reference input. Thus, the parameter adaptation mechanism has difficulty distinguishing parameter information from noise. Therefore, the parameter drift in the direction along with the tracking error remain small. In addition, the whole system could become unstable when the estimated parameter drifts to a point where the closed loop poles enter the right half complex plane.

In presence of measurements noise signal $\left(n(t)\right)$, the function $\bar{\boldsymbol{\Phi}}$ and $\boldsymbol{W}$ defined in (19) and (25) respectively could be rewritten as:

$$\bar{\boldsymbol{\Phi}} \to \bar{\boldsymbol{\Phi}} + \boldsymbol{n}(\boldsymbol{t})$$
$$\boldsymbol{q_2} \to \boldsymbol{q_2} + \boldsymbol{n}(\boldsymbol{t}) \quad (40)$$

Thus, if we toke the first part of the adaptation law (38) it will become:

$$\begin{aligned} \bar{\boldsymbol{\Phi}}^T \boldsymbol{s_2} &= \left(\bar{\boldsymbol{\Phi}}^T + \boldsymbol{n}(\boldsymbol{t})\right)\left(\boldsymbol{q_2} + \boldsymbol{n}(\boldsymbol{t}) - \boldsymbol{q_{2_d}}\right) \\ &= \bar{\boldsymbol{\Phi}}^T\left(\boldsymbol{q_2} - \boldsymbol{q_{2_d}}\right) + \boldsymbol{n}(\boldsymbol{t})\left(\bar{\boldsymbol{\Phi}}^T + \left(\boldsymbol{q_2} - \boldsymbol{q_{2_d}}\right)\right) \\ &\quad + \boldsymbol{n}(\boldsymbol{t})^2 \end{aligned} \quad (41)$$

From the equation above, it is easy to realize the noise effects on the adaptation law. Where the first term contains the parameter information and the second term tends to average out. However, the third term will cause parameter drifting which will make the parameter estimation drift away from the value of the true value.

5.1 Reducing Parameter Drift:

Reducing the parameter drift could be done by replacing the functions which contain the noise $\boldsymbol{n}(\boldsymbol{t})$, by the signals from the desired model $\boldsymbol{q_d}$ which are independent of the noise. This replacement must be done after the tracking error $(\boldsymbol{s_2})$ and the prediction error $(\boldsymbol{\epsilon})$ have converged well and their values have reduced within certain amount.

The adaptation law defined in (38) will be adjust according the errors values. For tracking error $(\boldsymbol{s_2})$:

$$\bar{\boldsymbol{\Phi}} = \begin{cases} \boldsymbol{Q}(\boldsymbol{q_r}) + \boldsymbol{F}\left(f_\phi, f_\theta, f_\psi, g\right) & |s_2| > \Delta \\ \boldsymbol{Q}(\boldsymbol{q_r}) + \boldsymbol{F}\left(f_{\phi_d}, f_{\theta_d}, f_{\psi_d}, g\right) & |s_2| \le \Delta \end{cases}$$

For prediction error $(\boldsymbol{\epsilon})$:

$$\boldsymbol{W} = \begin{cases} \lambda_f \left[\boldsymbol{Q}(\dot{\boldsymbol{q}}) - \dfrac{\lambda_f}{\Delta_f}\boldsymbol{Q}(\dot{\boldsymbol{q}}) + \dfrac{1}{\Delta_f}\boldsymbol{F}\right] & |\boldsymbol{\epsilon}| > \Delta \\ \lambda_f \left[\boldsymbol{Q}(\dot{\boldsymbol{q}}_d) - \dfrac{\lambda_f}{\Delta_f}\boldsymbol{Q}(\dot{\boldsymbol{q}}_d) + \dfrac{1}{\Delta_f}\boldsymbol{F_d}\right] & |\boldsymbol{\epsilon}| \le \Delta \end{cases}$$

6 SIMULATION RESULTS

A Simulation platform is benn devloped using Simulink software. The platform has been used to validate the proposed control algorithm and to illustrate the difference in behavior between the the robust and unrobust composite adaptive control. Figure 5 shows the used simulink platform.

In the simulation, all the plant parameters are considered to vary with time and they have been generated using square wave function. Also, they have a common duty cycle of 50% and a common frequency of $5\text{x}10^{-4}$ Hz. Still, each parameter has got different amplitude and offset which are shown in Table 1.

Table 1: Plant Parameters

Time Varying Parameter	Frequency in Hz	Offset	Amplitude
m	$5\text{x}10^{-4}$	1.5	1
I_x	$5\text{x}10^{-4}$	0.01	0.005
I_y	$5\text{x}10^{-4}$	0.0125	0.005
I_z	$5\text{x}10^{-4}$	0.02	0.01
k	$5\text{x}10^{-4}$	0.1	0.09
d	$5\text{x}10^{-4}$	0.002	0.001
Fixed Parameter	Value		
l	0.03		
J_p	$104\text{x}10^{-6}$		

The command signals $[x_c, y_c, z_c, \psi_c]$ are shown in Table 2. They have been generated using square wave function with a common duty cycle of 50%, amplitude of one and zero offsets. However they have different frequencies.

Table 2: Command Signal

Command	Frequency in Hz	Offset
x_c	0.015	0
y_c	0.01	0
z_c	0.012	0
ψ_c	0.009	0

in Table 3, illistrate the control parameters, which have been selected to satisfy the desired performance. And Table 4 shows the parameters estimation Mean Square Error (MSE), where robust adaptive control has got lower MSE in all parameters.

Table 3: Control Parameter

Parameter	Value
$\boldsymbol{A}_{m1}$	$\begin{bmatrix} -2 & 0 & -2 & 0 \\ 0 & -2 & 0 & -2 \\ 1 & 0 & 0 & 0 \\ 0 & 1 & 0 & 0 \end{bmatrix}$
$\boldsymbol{B}_{m1}$	$\begin{bmatrix} 2 & 0 \\ 0 & 2 \\ 0 & 0 \\ 0 & 0 \end{bmatrix}$
$\boldsymbol{\Lambda}_1$	eye(2)
$\boldsymbol{K}_1$	2 eye(2)
$\boldsymbol{A}_{m2}$	$\begin{bmatrix} \mathbf{a}_{11} & \mathbf{a}_{22} \\ \mathbf{I}_{4\text{x}4} & \mathbf{0}_{4\text{x}4} \end{bmatrix}$
$\boldsymbol{a}_{11}$	$diag([-2,-10,-10,-2])$
$\boldsymbol{a}_{22}$	$-diag([2,29,29,2])$
$\boldsymbol{B}_{m2}$	$\begin{bmatrix} \boldsymbol{a}_{22} \\ \mathbf{0}_{4\text{x}4} \end{bmatrix}$
$\boldsymbol{\Lambda}_2$	5 eye(4)
$\boldsymbol{K}_2$	6 eye(4)
P	$diag(1,1,1,1,5,5)$
$\boldsymbol{\lambda}_f$	20

Uniformly distributed random signals, which represent the noise, have been added to the states of the system and generated by the Simulink's blook. The noise has got zero mean value and ± 0.5 wight with different seeds. The noise represents the error in the sensor's measurment. The next figures show the results of the simulation test, where the robust composite adaptive control has better noise rejection than the unrobust one. The blue line , in the figures, represents the robust composite adaptive control and red one represents the non-robust one.

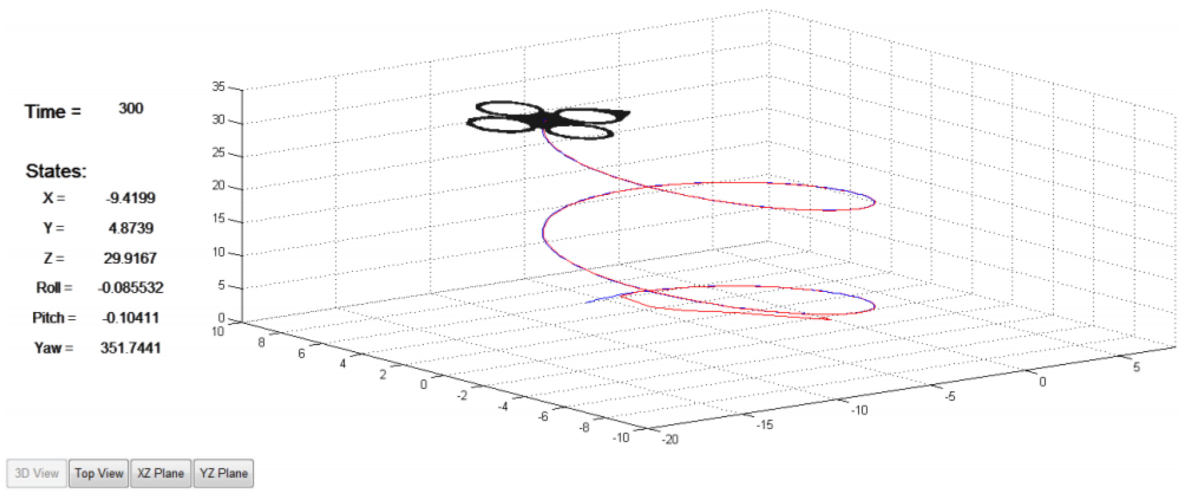

Figure 5: Simulation Platform

In Figure 6, the tracking error of the both scheme is illustrated. The robust control which has been represented in the blue line has less tracking error.

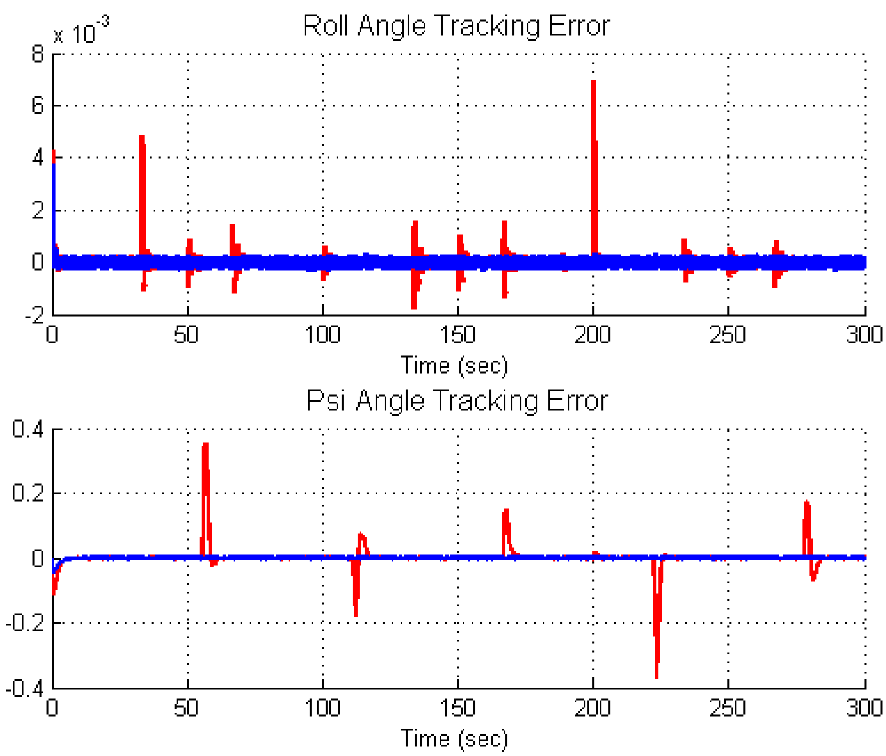

Figure 6: Tracking Error

In Figure 8, the parameter estimation has been plotted. The black thick line represents the true parameter estimation. The robust control has better ability to estimate the actual parameter.

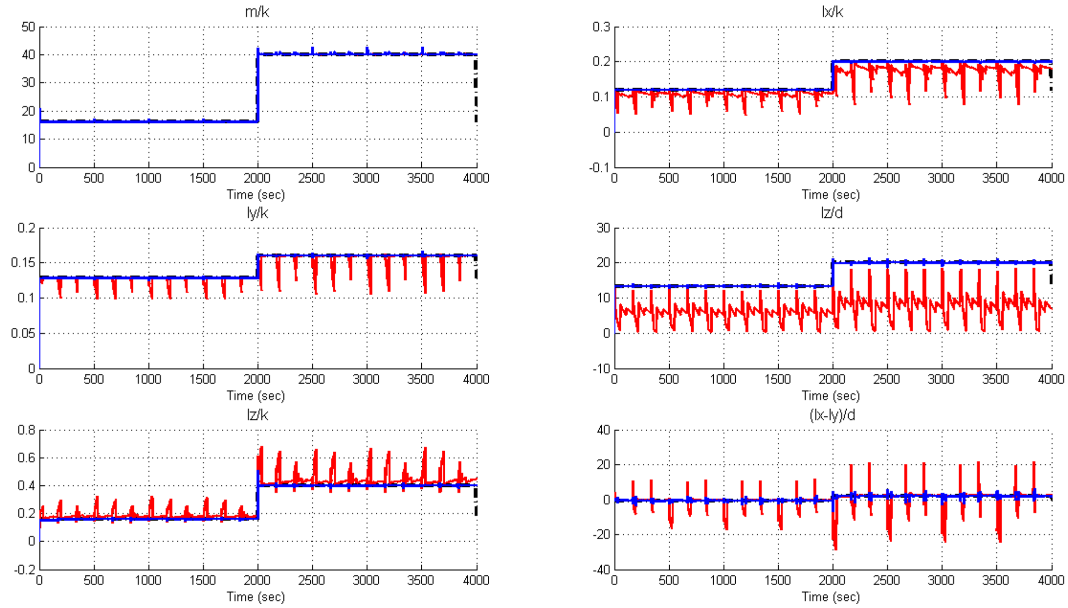

Figure 7: Parameter Estimation

In Figure 8, it is easily shown that the robust control can reject the noise in effective way.

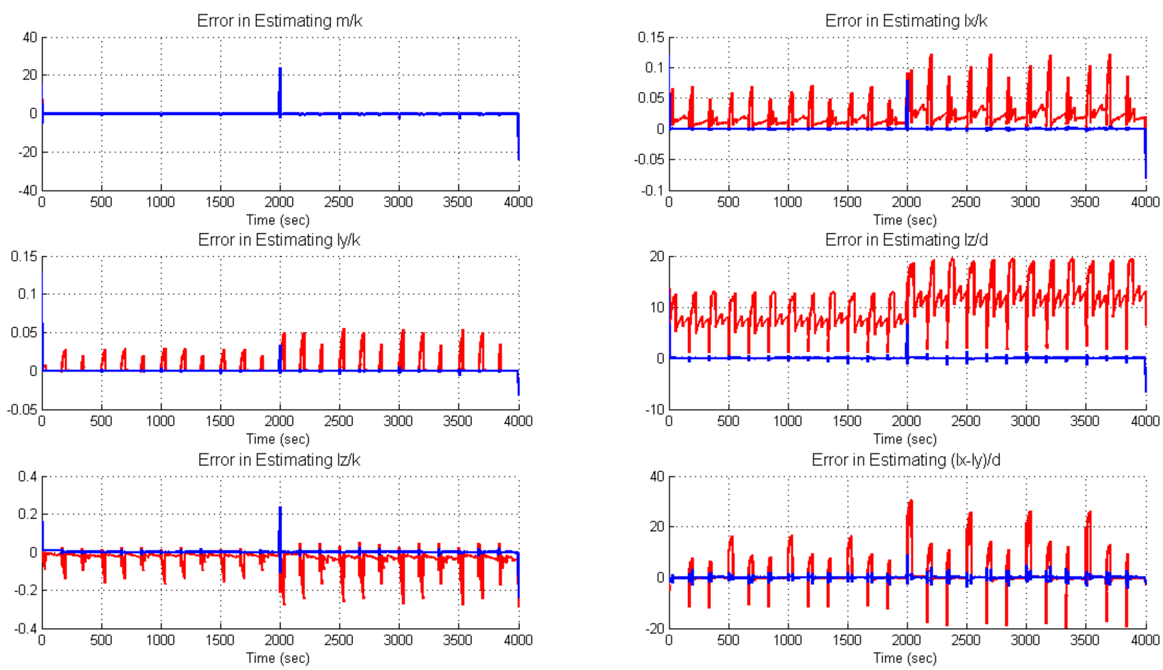

Figure 8: Parameters Error

Table 4: Parameter Estimation Mean Square Error (MSE)

Parameter	Method	
	Robust	Non-robust
m/k	0.10981	0.036170
I_x/k	0.00367	2.539e-05
I_y/k	0.01143	8.021e-05
I_z/d	22.8098	0.271159
I_z/k	0.06901	0.001622
$(I_x - I_y)/d$	2.51034	0.094554
m/k	0.10981	0.036170

CONCLUSION

A robust nonlinear composite adaptive control algorithm is done for a 6-DOF quadrotor system. The proposed controller forced the quadrotor to follow a desired position, velocity, acceleration and the heading angle despite the parameter uncertainty and noisy signal.

The composite adaptive controller is driven using the information from both the tracking errors and the parameter errors. The composite adaptive controller has been enhanced to reject the noise using robust technique. The stability of the closed-loop system is shown in the flight region of interest. Also the comparisons between both sachems are illustrated.

REFERENCES

[1] Puri, A. "A Survey of Unmanned Aerial Vehicles (UAV) for Traffic Surveillance." Technical Report, Tampa, 2005.

[2] Li, B., Mu, C. and Wu, B. "A Survey of Vision Based Autonomous Aerial Refueling forUnmanned Aerial Vehicles." Third International Conference on Intelligent Control and Information Processing. Dalian, China: IEEE, 2012.

[3] Saggiani, G. M., and Teodorani."Rotary wing UAV potential applications: an analytical study through a matrix method", Aircraft Engineering and Aerospace Technology, Vol. 76 Iss: 1, pp.6 – 14, 2004.

[4] Chowdhary, G., Sobers, M., Pravitra, C., Christmann, C., Wu, A., Hashimoto, H., Ong, C., Alghatgi, R. and Johnson, E. “Integrated Guidance Navigation and Control for a Fully Autonomous Indoor UAS.” AIAA Guidance Navigation and Control Conference, Portland, OR, August, 2011.

[5] Stevens, B. L. and Lewis, F. L. "Aircraft Control and Simulation. " Hoboken, New Jersey: John Wiley & Sons, Inc., 2nd ed., 2003.

[6] Huang, M., Xian, B., Diao, C., Yang, K. and Feng Y., "Adaptive Tracking Control Of Under-actuated Quadrotor Unmanned Aerial Vehicles Via Backstepping", In Proc. American Control Conference, Baltimore, USA, 2010., pp. 2076.

[7] Fang, Z. and Gao, W. 2011, "Adaptive integral backstepping control of a Micro-Quadrotor", IEEE, pp. 910.

[8] Min, B.-C., Hong, J.-H., and Matson, E., “Adaptive Robust Control (ARC) For An Altitude Control Of A Quadrotor Type UAV Carrying An Unknown Payloads,” in 2011 11th International Conference on Control, Automation and Systems (ICCAS), Oct. 2011, pp. 1147 –1151.

[9] Mohammadi, M.; Shahri, A.M., "Decentralized adaptive stabilization control for a quadrotor UAV," Robotics and Mechatronics (ICRoM), 2013 First RSI/ISM International Conference on , vol., no., pp.288,292, 13-15 Feb. 2013

[10] Schreier, M. 2012, "Modeling and adaptive control of a quadrotor", IEEE, , pp. 383.

[11] Fernando, T., Chandiramani, J., Lee, T. & Gutierrez, H. 2011, "Robust adaptive geometric tracking controls on SO(3) with an application to the attitude dynamics of a quadrotor UAV", IEEE, , pp. 7380.

[12] Imran Rashid, M. and Akhtar, S. 2012, "Adaptive control of a quadrotor with unknown model parameters", IEEE, pp. 8.

[13] Diao, C., Xian, B., Yin, Q., Zeng, W., Li, H. and Yang, Y., 2011, "A nonlinear adaptive control approach for quadrotor UAVs", IEEE, pp. 223.

[14] Dydek, Z.T., Annaswamy, A.M. and Lavretsky, E. 2013, "Adaptive Control of Quadrotor UAVs: A Design Trade Study With

Flight Evaluations", IEEE Transactions on Control Systems Technology, vol. 21, no. 4, pp. 1400-1406.

[15] Bialy, B.J., Klotz, J., Brink, K. & Dixon, W.E. 2013, "Lyapunov-based robust adaptive control of a quadrotor UAV in the presence of modeling uncertainties", IEEE, , pp. 13.

[16] Bouadi, H., Simoes Cunha, S., Drouin, A. & Mora-Camino, F. 2011, "Adaptive sliding mode control for quadrotor attitude stabilization and altitude tracking", IEEE, , pp. 449.

[17] Lee, D., Nataraj, C., Burg, T.C. and Dawson, D.M. 2011, "Adaptive tracking control of an underactuated aerial vehicle", IEEE, , pp. 2326.

[18] Das, A., Lewis, F. L., and Subbarao, K., "Sliding Mode Approach to Control Quadrotor Using Dynamic Inversion, Challenges and Paradigms in Applied Robust Control", ISBN: 978-953-307-338-5, InTech, DOI: 10.5772/16599. Available from: http://www.intechopen.com/books/challenges-and-paradigms-in-applied-robust-control/sliding-mode-approach-to-control-quadrotor-using-dynamic-inversion

[19] Sastry, S.S. and Isidore, A., "Adaptive Control of Linearizable Systems", I.E.E.E Transactions Automation Control, 1989.

[20] Slotine, J.J.E., and Coetsee, J.A., "Adaptive Sliding Controller Synthesis for Nonlinear Systems", Int. J. Control, 43(4), 1986.

[21] Slotine, J -J E, and Weiping Li. Applied Nonlinear Control. Englewood Cliffs, N.J. Prentice Hall, 1990., 1990.

[22] Emran, B. J., and A. Yesildirek. "NONLINEAR COMPOSITE ADAPTIVE CONTROL FOR QUADROTOR." *The International Conference on Electrical and Electronics Engineering, Clean Energy and Green Computing.* UAE: SDIWC, pp. 220-231, 2013.